

Polymer Microvascular Network Composites

S. C. OLUGEBEFOLA,¹ A. M. ARAGÓN,² C. J. HANSEN,³ A. R. HAMILTON,⁴
B. D. KOZOLA,⁵ W. WU,³ P. H. GEUBELLE,^{1,5} J. A. LEWIS,^{1,3}
N. R. SOTTOS^{1,3} AND S. R. WHITE^{1,5,*}

¹*Beckman Institute of Advanced Science and Technology, University of Illinois at Urbana-Champaign, Urbana, IL 61801, USA*

²*Department of Civil and Environmental Engineering, University of Illinois at Urbana-Champaign, Urbana, IL 61801, USA*

³*Department of Materials Science and Engineering, University of Illinois at Urbana-Champaign, Urbana, IL 61801, USA*

⁴*Department of Mechanical Science and Engineering, University of Illinois at Urbana-Champaign, Urbana, IL 61801, USA*

⁵*Department of Aerospace Engineering, University of Illinois at Urbana-Champaign, Urbana, IL 61801, USA*

ABSTRACT: Microvascular networks show promise for applications such as self-healing, self-cooling, and structural damage sensing. Fluid-filled micro-scale channels have been investigated extensively in the field of microfluidics, but three-dimensional networks in polymeric structural materials have been achieved only recently. The purpose of microvascular network integration is to provide a vehicle for the distribution and replenishment of active fluids throughout a matrix material enabling multifunctional operation. This perspective seeks to examine the advances in fabrication techniques, characterization, and new theoretical and computational tools for guiding design that are leading to systems with greater functionality and complexity.

KEY WORDS: microvascular, network, microchannels, self-cooling, optimization, 3D, direct-write, biomimetic, micromachining, self-healing.

INTRODUCTION

RECENT ADVANCES IN fabrication techniques at smaller length scales have generated interest in employing biomimicry to make new functional materials. The ability to make structures with hierarchical order similar to biological systems means that we can

*Author to whom correspondence should be addressed. E-mail: swhite@illinois.edu
Figures 1–5 appear in color online: <http://jcm.sagepub.com>

look to those same systems for solutions to emerging technical challenges. Microvascular systems are a prime example of the application of a biological solution to long-standing problems within structural materials. Vasculature primarily serves one purpose within complex biological organisms – transport of functional fluids to relevant tissues. However, within that framework there are many functions, such as delivery of nutrients and removal of waste, temperature regulation, and damage inhibition and repair. In the same way, the potential for synthetic microvascular systems lies within the ability to transport functional fluids within a material to effect changes to that material. This is a subtle distinction from the more general and widely studied field of microfluidics, where the emphasis is frequently on effecting changes within a fluid (e.g., performing chemical reactions) and the matrix serves primarily as a confinement for the manipulation of that fluid. In fact, there are several instances where the two fields overlap, especially in relation to fabrication techniques.

The basic concept for these systems is the introduction of microchannels – with diameters ranging from 1 micron to 1 mm – within a polymer, or polymer composite. Fluid can then be introduced into these channels to provide added functionality to the matrix material either by pumping, or taking advantage of capillary forces. Microvascular composites offer the benefits of added functionality and increased autonomy, namely, the ability to distribute active or reactive fluids for interactions with the matrix in regions traditionally difficult or impossible to reach in monolithic materials.

Currently, the applications that have received the most attention are in the areas of self-healing and active cooling. Self-healing microvascular systems employ the use of functional fluids as healing agents, usually monomeric formulations that can polymerize within an area of damage, or some combination of monomer and catalytic agent. The creation of new healed material restores the structural integrity of the matrix. Active cooling microvascular systems continuously circulate a fluid into, through, and out of the matrix in order to absorb and remove excess heat. The design of a microvascular network is highly dependent on a number of factors including the application, the properties of the matrix and the fluids, and the distribution method. Researchers have explored many aspects of these hybrid materials, both from a theoretical standpoint as well as approaches to fabrication and properties characterization. Much of the research discussed in this article is focused on the systems with channel diameters at the microscale, due to the unique advantages that this intermediate regime offers in terms of functionality. Nanoscale-channel diameters make fluid distribution difficult, especially at higher viscosities. In addition, the creation of macroscale networks with nanoscale features is at present difficult and somewhat impractical.

Finally, the presence of a microvascular network requires consideration of its effects on the materials' structural integrity both due to the absence of what would otherwise be load-bearing material replaced by the channels, and the compatibility between the fluid medium and the matrix itself. The expansiveness of the network must be balanced to maximize the benefit of the network, while minimizing the negative structural impact. There are several examples of structural (load bearing) biological tissues or materials that successfully incorporate microvasculature while maintaining robust mechanical properties, primarily due to exquisite control over the local micro- and nanostructure. Examination of these materials can lead to insight for future design of more effective microvascular composite materials.

BIOLOGICAL EXAMPLES

Biological materials such as dentin and bone possess toughness and strength significantly higher than their primary constituents, polymeric collagen fibrils and hydroxyapatite nanocrystals [1]. This robustness is attributed to the complex structural hierarchies that allow the matrix to benefit from the favorable properties of each material, the plasticity of the biopolymer, and the high tensile strength of the mineral component. Furthermore, both of these materials are highly vascularized and as such, there are specific morphological features near embedded channels whose primary purpose is to mitigate the adverse effects from the presence of the network.

Dentin is a natural composite material that makes up the bulk of human teeth below the enamel layer. It contains a high density of cylindrical tubules one to two micrometers in diameter that extend from the pulp to the enamel, roughly parallel to one another (Figure 1(a)). The tubules are sheathed in a ring of highly mineralized peritubular dentin within a bulk matrix of intertubular dentin. Balooch et al. [2] have estimated that the mineralization of the peritubular dentin results in an increase in compressive modulus from 17–23 GPa to 40–50 GPa. Nalla et al. [3] identified and estimated the relative effects of various mechanisms contributing to dentin's high fracture toughness by observing notch-induced crack initiation and growth. The creation of microcracks within the matrix and the peritubular regions was determined as one of the major extrinsic toughening mechanisms, along with crack bridging by collagen fibrils. Significantly, the reinforced tubules did not appear to deflect the crack tip, or influence the direction of crack propagation [4], suggesting the neutralizing effect of reinforcement on local stress concentrations.

Cortical bone, which makes up a large percentage of the load-bearing tissue in bones throughout the body, has been extensively studied for its excellent mechanical properties and complex hierarchical structure. Similar to dentin, it is made up of collagen fibers impregnated with apatite crystals. While bone is vascularized, in contrast to dentin, there is a more complex structure surrounding that vasculature. Each (Haversian) canal within cortical bone runs longitudinally to the bone long axis and is surrounded by an osteon made of many concentrically oriented 3–5 μm thick lamellar regions of compact tissue (Figure 1(b)) [5]. Work done by Götzen et al. [6] found that similar channels in equine cortical bone are surrounded by a region of low stiffness (as low as 2 GPa), then a region of high stiffness (up to 22 GPa), and then a far-field region of intermediate stiffness (10–13 GPa). The authors posit that this distribution of properties shifts peak stresses away from the edge of the channel and may explain some of the fracture behavior observed in the bone.

Studies on the fracture of bone [7,8] show that cracks tend to avoid the Haversian canals, following instead the line between osteons [7]. Microcracking in bone occurs preferentially around, between and at the lamellar interfaces within osteons; not at the edge of the canals [9]. Crack bridging by collagen fibrils here also serves as an important toughening mechanism.

The functional benefits of vascularization in load-bearing biomaterials are significant. The distribution of fluid between cells for nutrition and signaling allows these materials to support cellular processes for damage sensing and tissue repair, without compromising the structural function of the material. In the same way, various researchers seek to achieve

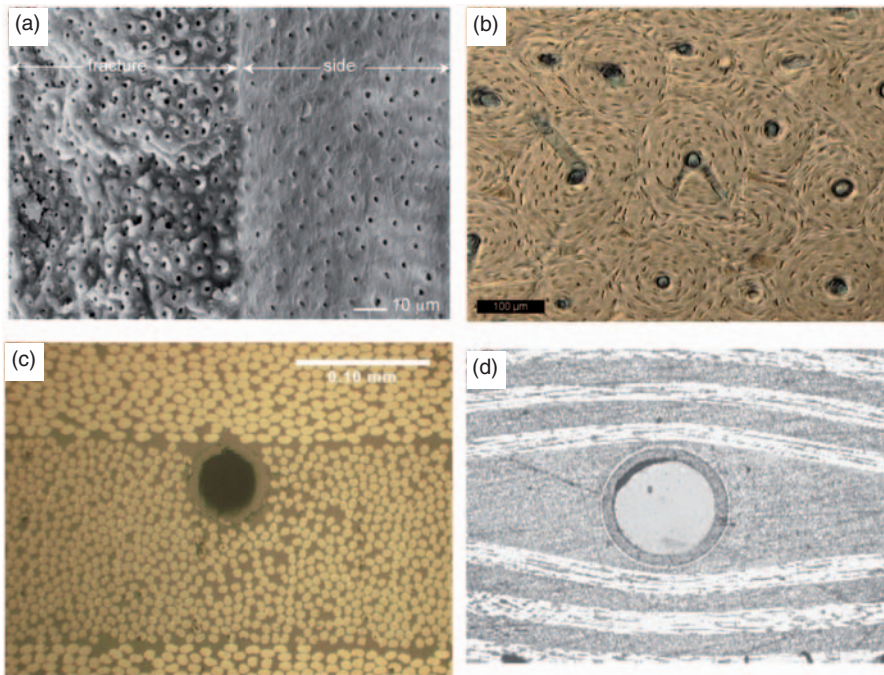


Figure 1. Microstructural examples from biological and synthetic vascular systems. (a) Section of dentin fracture plane showing tubule morphology [4]. (© Wiley-VCH Verlag GmbH & Co. KGaA. Reproduced with permission.) (b) Osteonal bone cross-section with Haversian canals surrounded by concentric osteonal lamellae [6]. (c) Glass-fiber composite with integrated fluid carrying fibers for self-healing and damage sensing [34]. (d) Air-filled glass tube in laminate composite structure for damage sensing [35]. (Reprinted with permission from Elsevier.).

this balance of enhanced function from the presence of a functional fluid and the maintenance of matrix properties through control of the microstructure near channel interfaces as well as the rational design of network architectures.

NETWORK DESIGN

Design Principles

While most microvascular network designs are constrained by the choices of fabrication method and materials, there remains a great deal of freedom in determining factors such as channel diameter, degree of branching, location of branch points, channel orientation, and others. Depending on the application, the optimal network architecture can vary significantly, but there are several parameters that apply to most systems. Some of these criteria are included here, as detailed in the literature [10,11].

PUMPING OPTIMIZATION

In general, if small microchannels and high flow rates are a requirement for a microvascular network, pumping optimization will be an important consideration. Fluid flow

through a microvascular network requires pumping power, which is dependent on the network resistance to flow. In considering biological optimization of microvascular flow in animals, Murray [12] considered two costs: the cost to pump fluid, which increases with smaller channels according to Poiseuille's Law, and the metabolic cost of blood, which increases proportionately with blood volume. The optimization, known as Murray's law is given by:

$$\sum r_p^3 = \sum r_d^3, \quad (1)$$

where r_p is the radius of the parent branch and r_d the radii of the daughter branches [12]. Biological studies have shown general agreement with Murray's Law [13,14]. Subsequent studies have demonstrated that close to the Murray's Law optimum, pumping power does not change dramatically, such that a 10% change in radius yields an increase in pumping power of only 3–5% [15,16].

While Murray's Law, which assumes a non-pulsatile flow, is valid for smaller branches within mammalian microvascular systems (e.g., arterioles), this agreement breaks down for larger branches (e.g., arteries) [17]. For branches higher up the hierarchy and nearer to a pulsatile pump, the pulsatile flow creates a dampened traveling wave that causes the microvascular network impedance to deviate from Murray's Law. Optimization of flow in the pulsatile case yields an area-preserving relationship:

$$\sum r_p^2 = \sum r_d^2, \quad (2)$$

where r_p and r_d are the same as in Equation (1). At smaller branches, viscosity effects again dominate the flow resistances and application of Murray's Law is recovered. Thus, design of microvascular networks depends upon the fluid flow conditions and the level of hierarchical branching.

SPATIAL OPTIMIZATION

Many microvascular network applications, such as self-healing and active cooling, would ideally contain volume-filling networks. However, vascular networks can adversely affect the structural properties of a material. This is particularly relevant to composite materials designed for demanding mechanical performance.

Optimization of the network location may mitigate adverse mechanical effects. Sandwich composite structures composed of fiber-reinforced skins separated by a core of rigid foam are one example. Microvascular networks can be placed in the core foam, such that the sandwich composite has an area-filling network without compromising the flexural stiffness of the overall composite [10].

Networks also impart stress concentrations to the overall structure. Shape factor can strongly influence the stress concentration, such that circular cross-sections are preferred over polygonal shapes with sharp angles. Stress fields are also affected by the spacing between neighboring vessels [18].

RELIABILITY OPTIMIZATION

In systems where the microvascular network provides a critical function, reliability is an important consideration. A system comprised of independent parallel components will have a probability of failure given by:

$$p = p_{\text{component}}^n, \quad (3)$$

where p is the system probability of failure, n the number of independent parallel components, and $p_{\text{component}}$ the failure probability of a single component [11]. Addition of duplicate components, such as pumps, will raise the total mass of the system and change the optimum radii of the network to achieve minimum system mass.

All these design principles focus on either optimization of network function or optimization of the network against failure. Network function may be optimized with regard to pumping or spatial distribution (as above), or with regard to healing, temperature control, or damage sensing. Protection against failure may be optimized with regard to pump failures, to fluid leaks, to blocked vessels, and to degradation of functional fluids over the component lifetime [11]. Both these optimization directions involve complex trade-offs requiring detailed knowledge of which functions and failure modes are critical. Moreover, these trade-offs are highly dependent on the end application.

For instance, the pumping and spatial distribution optimizations detailed above will depend on the system. In structural materials, minimization of the void volume and choice of a cross-sectional shape that minimizes stress concentrations are critical microvascular network design parameters. In order to meet these structural demands, pumping demands may be increased and network redundancy (and spatial distribution) may be reduced. Conversely, in a non-structural component cooled with a microvascular network, circulatory concerns are most important, so that using larger channels will reduce pumping power and greater network spatial distribution will increase total heat transfer. However, such a network will compromise the ultimate structural properties of the system.

Computational Design and Optimization

As a result of the large number of design variables associated with microvascular networks, optimization lends itself to computational approaches. Several methods have been proposed including (1) semi-analytical approaches; (2) gradient-based search methods; and (3) evolutionary algorithms (EAs).

Bejan and Lorente [19] have introduced the idea of constructal theory as a method of optimizing microvascular networks. The premise behind the theory is that flow systems tend to reach optimum delivery configurations over time. Researchers have used this approach for the example of channel coverage of defects in self-healing applications, examining the effects of both channel orientation, and simultaneous presence of two channel diameters [20]. By modeling a crack as a circular defect in a two-dimensional (2D) grid of channels with various regular geometric loop shapes, they determined that triangular grid sections aided crack filling with optimal coverage and determined the optimal ratio of channel diameters based on defect size. Kim et al. [21] examined the coverage ability of matched, branched network architectures (Figure 2(a)). Results indicated that having a single stream that branched was optimal relative to several smaller streams for covering clusters of subvolumes. Semi-analytical approaches such as constructal theory can be used to solve network optimization problems that do not involve a large set of optimization variables. These methods often require *a priori* information about the optimal solution.

Gradient-based optimization techniques iterate toward optimal solutions to problems or functions by approximating the local gradient of the function and determining the variable iteration direction that leads to a more optimized state. Within the gradient-based optimization techniques, topology optimization has been used to optimize flow networks [22]. Figure 2(b) shows a three-dimensional (3D) spherical arterial tree network with prescribed pressure at two nodes. As with most gradient-based search techniques, it involves design

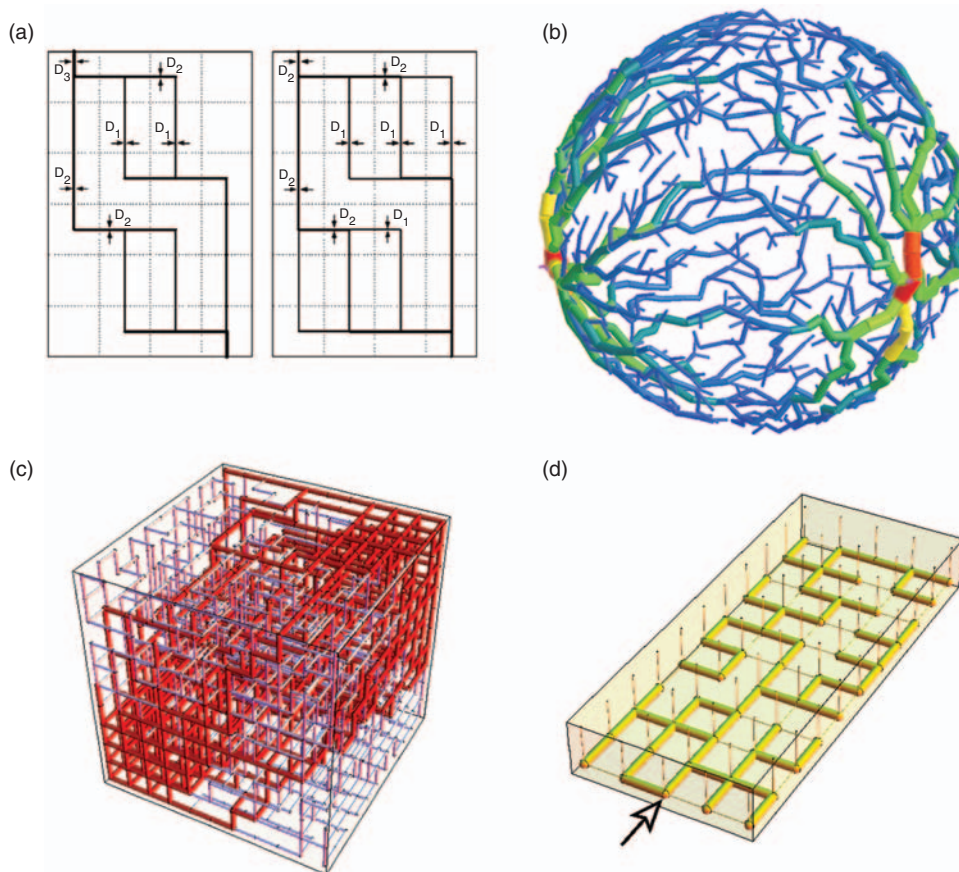


Figure 2. Examples of computational design methods for microvascular network design. (a) Two tree networks with two levels of branching joined canopy to canopy with channel diameters optimized for minimum flow resistance using constructal theory (Network 1 $D_1/D_2=0.827$ and $D_2/D_3=0.762$. Network 2 $D_1/D_2=0.682$). Reprinted with permission from [20]. (© 2006, American Institute of Physics.) (b) Arterial 3D flow network path for two input nodes determined by gradient-based optimization [22]. (c) 3D microvascular network optimized for flow efficiency and reduced volume fraction. Inlet and outlet are located at the lower left and upper right corners, respectively [25]. (d) 3D microvascular network optimization based on the self-healing coating experiment shown in Figure 5(a). This structure achieves the most uniform outflow to the upper surface [25]. (Reprinted with permission from Elsevier.).

variables that are continuous and lead to a solution that is likely to be a local optimum; so finding a global optimal solution is not guaranteed. In addition, due to the nature of the approach, it can only be used for objective functions for which a gradient can be computed.

EAs are population-based algorithms that improve a set of candidate solutions throughout their evolution. Genetic algorithms (GAs) [23,24] are the most widely known methodology of this group and use *selection*, *crossover*, and *mutation* as genetic operators to obtain better candidate solutions. The determination of the fittest individuals is done by the computation of one or more objective functions, which quantitatively describe how fit the individuals are to solve the problem. GAs can use discrete and/or continuous variables, and they search the entire decision space, so that optimal solutions found are likely to be global optima. Furthermore, there is no need for *a priori* knowledge about the optimal

solutions, but this information can be used to obtain a starting population with those features (knowledge-based GAs).

Aragon et al. [25] have used a multi-objective GA to optimize 2D and 3D microvascular network structures, considering various objective functions and constraints. Figure 2(c) shows an optimized microvascular network, considering the void volume fraction and the flow efficiency as objective functions. The flow efficiency is obtained by measuring the maximum pressure drop between any two locations in the network. The algorithm was also used to optimize the topology of a microvascular network used in self-healing coating experiments [26], so that the healing agent is uniformly distributed to the coating surface while minimizing the energy needed to drive the flow. The resulting topology, shown in Figure 2(d), creates a distribution network at the bottom of the material with the highest possible diameter vertical channels that connect to the upper surface with the minimum diameter available. This technique is also used for the multi-physics optimization of actively cooled microvascular materials. An example of this study is illustrated in Figure 3, where the GA has been used for a multi-objective optimization of a cooling network of microchannels embedded in a rectangular domain, subjected to a uniform heat source and convective boundary conditions [27]. Figure 3(a) shows the grid-like template on which the network (composed of microchannels of 100 μm diameter) is to be defined, and the temperature field in the absence of a cooling fluid. The inflow and outflow locations are located in the middle of the left and right edges of the domain respectively. Three objective functions are considered in the minimization process: the maximum temperature in the domain, the maximum pressure drop (assuming Poiseuille flow through all microchannels), and the void volume fraction (defined as the relative projected area of the network). Figure 3(b) shows the optimized network that provides the lowest maximum temperature in the domain for a given mass flow rate, showing a serpentine-like pattern for the microchannels in the network.

There is a great deal of inherent parameter space when determining the nature of a microvascular network to be used for a particular application. While optimization can be determined for a material theoretically, the choice of many of these parameters is determined by the material and network fabrication method. The more versatile the fabrication, the greater the design freedom, which leads to networks more suited to performing optimally at whatever function the design merits.

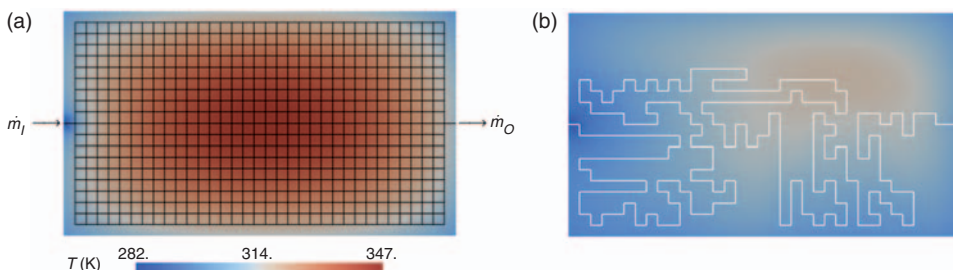


Figure 3. An active cooling network optimized using GA techniques. (a) Template microvascular network used as a starting configuration for the optimization algorithm superimposed over the temperature distribution in the absence of flow, where a uniform heat source is applied in the entire area and heat is lost by convection through the four edges. (b) Optimized microvascular network that reduces the maximum temperature in the domain, obtained using multi-objective GAs.

NETWORK FABRICATION AND APPLICATION

Microvascular network fabrication currently employs either discrete or interconnected channels, each of which has advantages and disadvantages. Discrete channels are generally easier to manufacture and in many cases can be fabricated independently from the matrix in which they are housed. In addition, premade channels can be loaded with whatever functional fluid is intended for use in the network prior to incorporation into the final material. By contrast, the creation of an interconnected network usually requires simultaneous fabrication with the surrounding matrix, increasing the process complexity, and necessitating compatibility between the manufacturing methods for the channels and the matrix.

Discrete Channel Arrays

Single channels can be manufactured and placed into a material in an array, in order to distribute functional fluids throughout that material without the flexibility and complication of creating interconnections. A large part of the network design considerations then relate to the appropriate spatial distribution of channels and the choice of channel diameters.

Early attempts to integrate a functional liquid phase in a solid material were made by embedding millimeter-scale diameter glass pipettes pre-filled with epoxy resin into bulk epoxies for the purpose of creating a self-healing material [28]. The channels in these cases were examined through optical and scanning electron microscopy of sample cross-sections before and after damage incurred through four-point bending tests. Motuku et al. [29] looked at glass millimeter-scale pipettes inserted into fiber-reinforced polymers (FRPs) for fluid release into damage areas. Initial studies focused on the structural effects of higher channel volume fraction on the matrix, a precursor to subsequent investigations with functional self-healing systems. Impact testing confirmed pipette breakage and fluid infiltration into damage areas, but no investigation into the self-healing properties of the composites was made. Importantly, these investigations were unconcerned with matrix/fluid compatibility prior to damage, as the fluid was enclosed within the glass channels alleviating any potential problems.

Glass and carbon fiber polymer composites are the most thoroughly explored materials for incorporation of discrete channel arrays. This is primarily due to the ease with which hollow fibers can be integrated into the fiber composite assembly process. Microscale filamentary channels for self-healing were initially investigated by Bleay et al. [30], making use of commercially available 15 μm diameter glass fibers to create a unidirectional pre-impregnated ply. These plies were stacked to create $[(0,90)_{12}]_s$ and $[(\pm 45,0,90)_6]_s$ composite laminates. Post-cure, the fibers were filled with liquid resin using vacuum-assisted capillary action. The authors began to address some of the pertinent factors concerning microvascular network incorporation, namely the effects of the fibers on the material structural integrity, methods for filling microscale fibers already embedded in the matrix, and the effective functionality of the fluid component in the channels, and in this case, the ability of the fluid to reach damage areas and effect strength recovery. The visualization of the channels *in situ* was accomplished using X-radiography with a contrast agent doped fluid. Significantly, the narrow internal diameter of the hollow fibers coupled with the high viscosity of the resin hindered the uptake of the resin into the fibers as well as its post-impact release into damaged regions. Compression testing after impact

showed that these two problems thwarted any potential self-healing effects, as 'healed' samples showed no more mechanical recovery than control samples with unfilled fibers.

Pang and Bond [31,32] fabricated 60- μm diameter hollow glass fibers with optimized void volume and incorporated both hollow and solid glass fiber plies into a hybrid laminate, with a $[(90,0)_{\text{solid}}, (90,0,90,0)_{\text{hollow}}, (90,0,90)_{\text{solid}}]_s$ stacking sequence. The increased hollowness of the fibers allowed easy filling using vacuum-assisted infiltration. A two-part fluid epoxy resin/hardener system was used to investigate self-healing capability, with each part separately loaded into perpendicularly oriented fiber arrays, designed to mix and cure only after being released into the damaged region. To add functionality to the system, a UV-fluorescent dye was incorporated with the resin to enable both fluid-filled fiber and damage visualization. Four-point bending tests post-indentation showed flexural strength recovery under some conditions, but the healing system possessed poor long-term activity, posited to be the result of the incorporation of solvent and other additives into the resin. Visualization of released fluid from the channels was quite successful, enabling clear and rapid delineation of the damage area when compared to more laborious characterization approaches, such as C-scan ultrasonography. Bond and coworkers [33,34] further explored the structural effects of hollow fiber channels through examination of simulated-impact damaged specimens with variations in lateral channel distribution. Network designs with smaller channel-to-channel distances were found to increase healing recovery of flexural strength, but conversely to reduce baseline strength along with modifying crack propagation behavior. The effects were partially attributed to poor uniformity of channel spacing during fabrication and to the replacement of some load-bearing carbon fiber material with the hollow fiber channels.

Kousourakis et al. [35,36] have also utilized discrete channel arrays for damage sensing in laminar composites through comparative vacuum monitoring. By integrating air-filled channels alternating between high and low pressure, any damage that spans two adjacent channels will detectably equalize their pressures. The authors examined the mechanical effects of incorporating both micro- and millimeter-scale hollow glass fibers, and empty channels created by inserting and removing space-filling polydimethylsiloxane (PDMS) mandrels. Microchannels were observed to increase mode I interlaminar fracture toughness when oriented normal to the crack propagation direction, with reduced additional enhancement at larger diameters. This mechanical improvement was attributed to crack blunting (empty, hollow fiber) and deflection (hollow fiber) mechanisms. A trade-off was found in that the interlaminar shear strength decreased linearly with increasing channel size. In addition, the authors determined that the tensile and compressive strengths and moduli decreased at critical channel diameters, as they approached the millimeter scale.

The potential for discrete channel arrays for use in damage reduction and detection is significant, but limited by the difficulty in replacing fluid to depleted channels. The need for each channel to fill specific damage volumes for complete self-healing places constraints on how sparsely the channels can be distributed, which affects mechanical properties. Creating interconnected networks reduces that constraint, while opening up additional applications for the network that take advantage of fluid flow, such as self-cooling.

Interconnected Networks

Greater control over the placement and orientation of channels in network architectures is one of the most important goals of this research. Customizing a network to a particular

matrix or shape will enable the fabrication of modular subsections with added functionality. While glass and carbon fiber composites are a convenient embedment material due to the similarity in shape between support fibers and channels, creating interconnected networks will necessarily involve a divergence from purely parallel arrays. In contrast to channel arrays, where hollow glass fibers are the dominant paradigm, there are several techniques that have been developed to fabricate interconnected networks, driven by applications in self-healing, but also self-cooling for integrated circuits (ICs) and microfluidics for chemistry and biology/bioengineering.

MACHINING AND ETCHING

Bond and coworkers [37,38] have created millimeter-scale vascular networks for self-healing within composite sandwich structures by laying down parallel polyvinyl chloride ‘supply vessels’ along the central plane of the core and drilling vertical risers through the thickness of the material followed by the application of the surface skins. The channel spacing was chosen to achieve reasonable areal coverage of the skin-core interface. Specimens that achieved good resin/hardener mixing showed full recovery of compression strength after impact [37].

Micromachining techniques have been used extensively to create microchannels for cooling applications in ceramics, metals, and polymers. The most basic form is to apply traditional machining principles at the microscale to create channel grooves. These types of systems have been utilized to create channels on the order of 600–700 μm in width and depth [39]. Current CNC machines utilizing electrical discharge machining (EDM) are capable of producing feature sizes on the order of tens of microns. [40] Laser micromachining can also be utilized to fabricate microchannels in a layer-by-layer fabrication approach, where the channel structure is written in a series of successive layers that are subsequently bonded together [41]. Current laser micromachining technology is capable of sub-micron resolution [42] and is well suited to fabricating precise microchannels. Figure 4(a) shows microchannels fabricated in polycarbonate via direct write laser ablation. This method creates V-shaped grooves, where the cross-section is determined by the laser power and writing speed (Figure 4(a)) [43].

Three-dimensional networks for cooling have been fabricated using chemical etching of silicon for close integration with IC components. Wei et al. [44] used stacked 2D manifolds to create two-layer networks with independently controllable flow directions. The authors

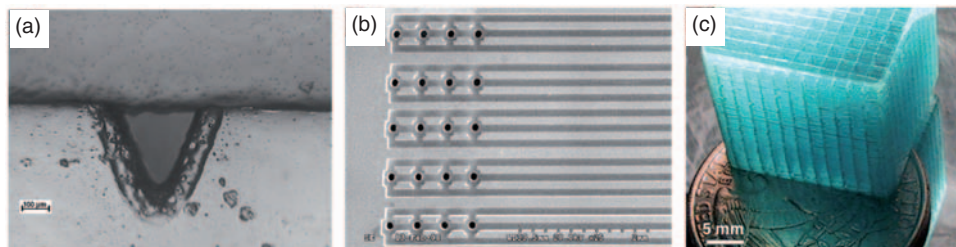


Figure 4. Microvascular networks formed by different fabrication methods. (a) Microchannel fabricated by laser ablation of a polycarbonate substrate [43]. (Reprinted with permission from Elsevier.) (b) SEM image of one layer of an integrated microchannel heat sink with fluidic through-silicon vias [45] (© 2008 IEEE). (c) 104-layer direct ink written microvascular network encased in a clear epoxy matrix [48]. (© Wiley-VCH Verlag GmbH & Co. KGaA. Reproduced with permission.).

noted several differences between the cooling profiles of the parallel flow and counterflow cases, notably increased thermal resistance, but better thermal uniformity at low flow rates for the counterflow case. King et al. [45] describe a complex method for creating 3D stacked die ICs etched in silicon with copper, and polymer component interconnects (Figure 4(b)). As opposed to most heat exchangers that are placed outside the relevant heat source, this technique puts the channels within and throughout the part, resulting in a truly integrated network.

Most of these techniques are versatile with respect to 2D patterning capability, but suffer the limitation of requiring stacking, and thus fine control over registration, to create 3D interconnected networks. For applications such as IC cooling where the matrix itself is carefully patterned, this is not as significant as an issue; but for other applications, these methods may be less practical. While the materials used for many of these techniques are commonly ceramic, or semiconductor based, the basic ideas could be straightforwardly applied to the creation of networks within polymeric systems.

FUGITIVE SCAFFOLD PROCESSES

The direct ink writing (DIW) technique involves the controlled extrusion of fugitive viscoelastic inks through a fine nozzle to build 3D structures [46]. The nozzle, mounted on a three-axis, robotically controlled stage permits fabrication of structures in a layer-by-layer approach. Interconnected, 3D microchannels are produced by first depositing an organic ink in a pre-defined pattern, then infiltrating the structure with a material, such as a two-part epoxy or photopolymer, that is subsequently cured to form a solid matrix. The fugitive ink is liquefied and removed from the matrix with application of modest vacuum, leaving behind the desired microchannel network (Figure 4(c)) [47,48].

Toohey et al. [26] used DIW to produce a system that schematically mimics the structure of skin, with an epoxy substrate containing a 3D vascular grid of microchannels filled with the monomeric fluid dicyclopentadiene (DCPD), and a surface coating with incorporated Grubbs' catalyst (Figure 5(a)). The fracture of the coating under four-point bending released the DCPD from the vertical channels into the crack plane, leading to contact with the catalyst and subsequent polymerization. Tests of the coatings after damage and healing showed partial recovery of fracture toughness. Most notably, due to the interconnected nature of the network, the monomer reservoir could be replenished, enabling up to

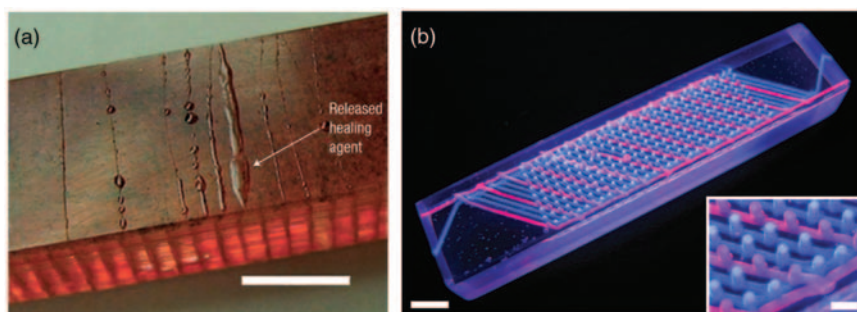


Figure 5. Examples of direct-write microvascular networks. (a) Grid network for surface coating self-healing (scale bar = 5 mm) [26]. (Adapted by permission from Macmillan Publishers Ltd.) (b) Interpenetrating network fabricated through direct-write assembly with dual inks. The networks are highlighted with red and blue fluorescent solutions (scale bar = 5 mm, inset scale bar = 2 mm).

seven consecutive healing events in a single sample. In an effort to extend the number of healing cycles, the researchers employed the DIW method to make single grids, and then utilized photo-polymerization to isolate separate networks for two-part epoxy healing schemes [49]. In contrast to similar healing systems used by Bond and coworkers, where the fluid was sealed within a glass fiber, the choice of resin and hardener required chemical compatibility tests with the matrix due to their direct contact at the channel surface. An appropriate two-part epoxy avoided swelling and cracking of the network matrix, extending the number of healing cycles to 16. The healing process was not indefinitely repeatable, due to build up of polymer in the crack plane from previous healing cycles. This healed polymer 'scar' prevented proper mixing of the fluid components, highlighting the importance of network geometry and fluid viscosities in controlling the network effectiveness.

Hansen et al. [50] achieved greater control over network architecture through the use of a dual ink writing method. The authors used microcrystalline wax ink that melts at high temperatures, as well as a block-copolymer ink that melts below room temperature. This advancement allowed the writing of complex, separate, and interpenetrating networks to aid the mixing of healing components (Figure 5(b)). By creating vertical channels from each network in a number ratio close to the ideal chemical stoichiometry of the epoxy and by decreasing the diffusion distances, the number of healing cycles was further extended beyond 30.

Kozola et al. [51] have also used DIW to make networks for active-cooling by creating thin fin polymer specimens with embedded channels with varying network geometries. Using infrared imaging, the researchers examined the effects of flow rate, channel diameter, dimensionality, and cooling fluid on the transition from the heated specimen in the absence of flow to the steady-state regime with flow as well as the effectiveness of steady-state cooling. Additionally, they applied micro-scale particle image velocimetry to measure flow rates in individual channels, in order to determine critical threshold flow rates for effective channel cooling.

Bellan et al. [52] have generated microvascular networks within PDMS, epoxy, and polycaprolactone matrices using melt-spun sugar fugitive scaffolds. While this technique is limited in the fine control of microchannel placement and diameter, it is readily scalable and relatively inexpensive to apply. Huang et al. [53] have generated microvascular networks within poly(methyl methacrylate) and poly(lactic acid) blocks with electron beam irradiation followed by rapid discharge. The resulting structures closely resemble biological vasculature in morphology and various properties of the networks such as the degree of branching and the number and location of entry and exit points can be loosely controlled.

FUTURE DIRECTIONS

The field of microvascular composites is poised to advance rapidly due to the recent advent of appropriate tools for both fabrication and design. There are some fundamental aspects of network design that still need further study, notably the investigation of structural changes caused by the presence of the network. While some systems have managed to mitigate their effects through minimizing network volume, the interaction between the matrix and the channel at the interface can also be potentially modified to aid in controlling adverse structural problems. In most discrete channel arrays of hollow fibers, there is a stiff glass layer at the interface between the network and the matrix, though the effects have not been optimized. Hamilton et al. [54] have shown that the strain concentrations of

a channel in an epoxy matrix under tensile load can be significantly reduced by deposition of a stiff alumina particulate layer at the channel interior surface. Similarly to biological responses to the presence of a channel network, modification of the mechanical properties near channel surfaces may lead to improved damage tolerance and toughness.

The ability to accurately determine optimal solutions given the constraints for a particular application through modeling, coupled with the ability to fabricate complex, integrated 3D networks, should enable multifunctional microvascular composites without sacrificing structural integrity. The next steps for increasing the applicability of these systems will be increasingly dependent on methods for easily constructing large-scale specimens that can be used to replace monolithic materials. For top-down assembly techniques such as the ones described previously, there may be a natural trade-off between the degree of control over network architecture and the difficulty in constructing said architecture.

While the microvascular network concept shows significant promise, in comparison to biological systems the current states of design and functionality are still very basic. Recent studies look at artificial systems designed for one type of application at a time, but complex biological vascular systems can support multiple functions – transporting nutrients to and removing waste from distributed tissues, storing, and delivering healing components, temperature regulation, signaling – without isolating, and usually without interference between the relevant agents. Up to this point, fluids used in synthetic microvasculature studies have been mostly homogeneous, optimized to function at most two ways (self-healing, damage visualization). In the future, the use of multifunctional mixtures may lead to greater efficiency and utility for these systems. Balazs and coworkers [55–57] have explored the use of self-segregating particles to autonomously heal cracks in polymer–semiconductor multilayer structures and similar particles within a functional fluid could lead to more advanced multifunctional systems.

In addition, the ability to control the fluid flow through microvascular networks has not yet been fully exploited. The modular nature of biological circulatory networks is a function of tissue remodeling processes on long-time scales, and constriction of flow from reduced vessel diameter on short-time scales. Incorporating valves and external stimuli-based autonomic behaviors into synthetic vascular systems can only increase their reliability and further expand their usefulness. Changing the direction of flow through different regions of a sample for modular cooling is just one example of the way in which these systems can yield new and interesting properties.

ACKNOWLEDGMENTS

The authors gratefully acknowledge the support for this research provided by AFOSR (MURI grant no. F49550-05-1-0346). C. Hansen is supported in part by an NSF Graduate Student Fellowship.

REFERENCES

1. Landis, W. (1995). The Strength of a Calcified Tissue Depends in Part on the Molecular-structure, Organization of its Constituent Mineral Crystals in their Organic Matrix, *Bone*, **16**(5): 533–544.
2. Balooch, G., Marshall, G.W., Marshall, S.J., Warren, O.L., Asif, S.A.S. and Balooch, M. (2004). Evaluation of a New Modulus Mapping Technique to Investigate Microstructural Features of Human Teeth, *Journal of Biomechanics*, **37**(8): 1223–1232.

3. Nalla, R.K., Kinney, J.H. and Ritchie, R.O. (2003). Effect of Orientation on the In Vitro Fracture Toughness of Dentin: The Role of Toughening Mechanisms, *Biomaterials*, **24**(22): 3955–3968.
4. Nalla, R.K., Kinney, J.H. and Ritchie, R.O. (2003). On the Fracture of Human Dentin: Is it Stress-or Strain-controlled?, *Journal of Biomedical Materials Research*, **67**(2): 484–495
5. Weiner, S., Traub, W. and Wagner, H. (1999). Lamellar Bone: Structure-Function Relations, *Journal of Structural Biology*, **126**(3): 241–255.
6. Götzen, N., Cross, A.R., Ifju, P.G. and Rapoff, A.J. (2003). Understanding Stress Concentration About a Nutrient Foramen, *Journal of Biomechanics*, **36**(10): 1511–1521.
7. Nalla, R., Kruzic, J., Kinney, J. and Ritchie, R. (2005). Mechanistic Aspects of Fracture and R-curve Behavior in Human Cortical Bone, *Biomaterials*, **26**(2): 217–231.
8. Nalla, R., Kinney, J. and Ritchie, R. (2003). Mechanistic Fracture Criteria for the Failure of Human Cortical Bone, *Nature Materials*, **2**(3): 164–168.
9. Ebacher, V. and Wang, R. (2009). A Unique Microcracking Process Associated with the Inelastic Deformation of Haversian Bone, *Advanced Functional Materials*, **19**(1): 57–66.
10. Williams, H.R., Trask, R.S., Weaver, P.M. and Bond, I.P. (2008). Minimum Mass Vascular Networks in Multifunctional Materials, *Journal of the Royal Society Interface*, **5**(18): 55–65.
11. Williams, H.R., Trask, R.S., Knights, A.C., Williams, E.R. and Bond, I.P. (2008). Biomimetic Reliability Strategies for Self-healing Vascular Networks in Engineering Materials, *Journal of the Royal Society Interface*, **5**(24): 735–747.
12. Murray, C.D. (1926). The Physiological Principle of Minimum Work II. Oxygen Exchange in Capillaries, *Proceedings of the National Academy of Sciences of the United States of America, USA*, **12**(5): 299–304.
13. Sherman, T. (1981). On Connecting Large Vessels to Small – the Meaning of Murray’s Law, *Journal of General Physiology*, **78**(4): 431–453.
14. Kassab, G. (2006). Scaling Laws of Vascular Trees: of Form and Function, *American Journal of Physiology. Heart and Circulatory Physiology*, **290**(2): H894–H903.
15. Milsum, J.H. and Roberge, F.A. (1973). Physiological Regulation and Control, In: Rosen, R. (ed.), *Foundations of Mathematical Biology*, pp. 86–92, Academic Press, New York, NY.
16. Sherman, T., Popel, A., Koller, A. and Johnson, P. (1989). The Cost of Departure from Optimal Radii in Microvascular Networks, *Journal of Theoretical Biology*, **136**(3): 245–265.
17. West, G., Brown, J. and Enquist, B. (1997). A General Model for the Origin of Allometric Scaling Laws in Biology, *Science*, **276**(5309): 122–126.
18. Rice, R. (1997). Limitations of Pore-stress Concentrations on the Mechanical Properties of Porous Materials, *Journal of Materials Science*, **32**(17): 4731–4736.
19. Bejan, A. and Lorente, S. (2006). Constructal Theory of Generation of Configuration in Nature and Engineering, *Journal of Applied Physics*, **100**(4): 041301.
20. Bejan, A., Lorente, S. and Wang, K. (2006). Networks of Channels for Self-healing Composite Materials, *Journal of Applied Physics*, **100**(3): 033528.
21. Kim, S., Lorente, S. and Bejan, A. (2006). Vascularized Materials: Tree-shaped Flow Architectures Matched Canopy to Canopy, *Journal of Applied Physics*, **100**(6): 063525.
22. Klarbring, A., Petersson, J., Torstenfelt, B. and Karlsson, M. (2003). Topology Optimization of Flow Networks, *Computer Methods in Applied Mechanics and Engineering*, **192**(35–36): 3909–3932.
23. Goldberg, D.E. (1989). *Genetic Algorithms in Search, Optimization, and Machine Learning*, **1st edn**, Addison-Wesley Professional, Upper Saddle River, NJ, USA.
24. Goldberg, D.E. (2002). *The Design of Innovation: Lessons from and for Competent Genetic Algorithms*, Springer, New York.
25. Aragon, A.M., Wayer, J.K., Geubelle, P.H., Goldberg, D.E. and White, S.R. (2008). Design of Microvascular Flow Networks Using Multi-objective Genetic Algorithms, *Computer Methods in Applied Mechanics and Engineering*, **197**(49–50): 4399–4410.
26. Toohey, K.S., Sottos, N.R., Lewis, J.A., Moore, J.S. and White, S.R. (2007). Self-healing Materials with Microvascular Networks, *Nature Materials*, **6**(8): 581–585.

27. Aragon, A.M., O'Rourke, B., Smith, K., Geubelle, P.H. and White, S.R. (2008). Multi-physics Optimization of Biomimetic Microvascular Materials, *Society of Engineering Science, 45th Annual Technical Meeting*, Urbana, IL.
28. Dry, C.M. (1996). Procedures Developed for Self-repair of Polymer Matrix Composite Materials, *Composite Structures*, **35**(3): 263–269.
29. Motuku, M., Vaidya, U.K. and Janowski, G.M. (1999). Parametric Studies on Self-repairing Approaches for Resin Infused Composites Subjected to Low Velocity Impact, *Smart Materials and Structures*, **8**(5): 623–638.
30. Bley, S.M., Loader, C.B., Hawyes, V.J., Humberstone, L. and Curtis, P.T. (2001). A Smart Repair System for Polymer Matrix Composites, *Composites Part A: Applied Science and Manufacturing*, **32**(12): 1767–1776.
31. Pang, J.W.C. and Bond, I.P. (2005). 'Bleeding composites' – Damage Detection and Self-repair using a Biomimetic Approach, *Composites Part A: Applied Science and Manufacturing*, **36**(2): 183–188.
32. Pang, J.W.C. and Bond, I.P. (2005). A Hollow Fibre Reinforced Polymer Composite Encompassing Self-healing and Enhanced Damage Visibility, *Composites Science and Technology*, **65**(11–12): 1791–1799.
33. Trask, R.S. and Bond, I.P. (2006). Biomimetic Self-healing of Advanced Composite Structures Using Hollow Glass Fibres, *Smart Materials and Structures*, **15**(3): 704–710.
34. Williams, G., Trask, R. and Bond, I. (2007). A Self-healing Carbon Fibre Reinforced Polymer for Aerospace Applications, *Composites Part A: Applied Science and Manufacturing*, **38**(6): 1525–1532.
35. Kousourakis, A., Mouritz, A.P. and Bannister, M.K. (2006). Interlaminar Properties of Polymer Laminates Containing Internal Sensor Cavities, *Composite Structures*, **75**(1–4): 610–618.
36. Kousourakis, A., Bannister, M.K. and Mouritz, A.P. (2008). Tensile and Compressive Properties of Polymer Laminates Containing Internal Sensor Cavities, *Composites Part A: Applied Science and Manufacturing*, **39**(9): 1394–1403.
37. Williams, H.R., Trask, R.S. and Bond, I.P. (2007). Self-healing Composite Sandwich Structures, *Smart Materials and Structures*, **16**(4): 1198–1207.
38. Williams, H.R., Trask, R.S. and Bond, I.P. (2008). Self-healing Sandwich Panels: Restoration of Compressive Strength After Impact, *Composites Science and Technology*, **68**(15–16): 3171–3177.
39. Peng, X. and Wang, B. (1993). Forced-Convection and Flow Boiling Heat-transfer for Liquid Flowing through Microchannels, *International Journal of Heat and Mass Transfer*, **36**(14): 3421–3427.
40. Chen, S. (2008). Fabrication of High-density Micro Holes by Upward Batch Micro EDM, *Journal of Micromechanics and Microengineering*[Internet]. Available at: http://apps.isiknowledge.com.proxy2.library.uiuc.edu/full_record.do?product=WOS&search_mode=GeneralSearch&qid=74&SID=1B905D5FCO3-KmpAOn4F&page=1&doc=1 (accessed January 23, 2010).
41. Paul, B., Kwon, P. and Subramanian, R. (2006). Understanding Limits on Fin Aspect Ratios in Counterflow Microchannel Arrays Produced by Diffusion Bonding, *Journal of Manufacturing Science and Engineering – Transactions of the ASME*, **128**(4): 977–983.
42. Saxena, I., Agrawal, A. and Joshi, S. (2009). Fabrication of Microfilters Using Excimer Laser Micromachining and Testing of Pressure Drop, *Journal of Micromechanics and Microengineering*[Internet]. Available at: http://apps.isiknowledge.com.proxy2.library.uiuc.edu/full_record.do?product=WOS&search_mode=GeneralSearch&qid=84&SID=1B905D5FCO3-KmpAOn4F&page=1&doc=1 (accessed January 23, 2010).
43. Qi, H., Chen, T., Yao, L. and Zuo, T. (2009). Micromachining of Microchannel on the Polycarbonate Substrate with CO₂ Laser Direct-writing Ablation, *Optics and Lasers in Engineering*, **47**(5): 594–598.
44. Wei, X., Joshi, Y. and Patterson, M. (2007). Experimental and Numerical Study of a Stacked Microchannel Heat Sink for Liquid Cooling of Microelectronic Devices, *Journal of Heat Transfer – Transactions of the ASME*, **129**(10): 1432–1444.

45. King, Jr. C.R., Sekar, D., Bakir, M.S., Dang, B., Pikarsky, J. and Meindl, J.D. (2008). 3D Stacking of Chips with Electrical and Microfluidic I/O Interconnects [Internet]. In: *2008 58th Electronic Components and Technology Conference, ECTC*, Institute of Electrical and Electronics Engineers Inc., Lake Buena Vista, FL, USA, 27–30 May, pp. 1–7. Available at: <http://dx.doi.org/10.1109/ECTC.2008.4549941> (accessed January 11, 2010).
46. Lewis, J. (2006). Direct Ink Writing of 3D Functional Materials, *Advanced Functional Materials*, **16**(17): 2193–2204.
47. Therriault, D., White, S. and Lewis, J. (2003). Chaotic Mixing in Three-dimensional Microvascular Networks Fabricated by Direct-write Assembly, *Nature Materials*, **2**(4): 265–271.
48. Therriault, D., Shepherd, R.F., White, S.R. and Lewis, J.A. (2005). Fugitive Inks for Direct-write Assembly of Three-dimensional Microvascular Networks, *Advanced Materials*, **17**(4): 395–399.
49. Toohey, K., Hansen, C., Lewis, J., White, S. and Sottos, N. (2009). Delivery of Two-part Self-healing Chemistry via Microvascular Networks, *Advanced Functional Materials*, **19**(9): 1399–1405.
50. Hansen, C.J., Wu, W., Toohey, K.S., Sottos, N.R., White, S.R. and Lewis, J.A. (2009). Self-healing Materials with Interpenetrating Microvascular Networks, *Advanced Materials*, **21**(41): 4143–4147.
51. Kozola, B.D., Natrajan, V.K., Christensen, K.T. and White, S.R. (2008). Active Cooling of Polymer Structures Using Microvascular Networks, In: *45th SES Technical Meeting*, University of Illinois at Urbana-Champaign, Urbana, IL.
52. Bellan, L.M., Singh, S.P., Henderson, P.W., Porri, T.J., Craighead, H.G. and Spector, J.A. (2009). Fabrication of an Artificial 3-Dimensional Vascular Network Using Sacrificial Sugar Structures, *Soft Matter*, **5**(7): 1354–1357.
53. Huang, J., Kim, J., Agrawal, N., Sudarsan, A.P., Maxim, J.E., Jayaraman, A. and Ugaz, V.M. (2009). Rapid Fabrication of Bio-inspired 3D Microfluidic Vascular Networks, *Advanced Materials*, **21**(35): 3567–3571.
54. Hamilton, A., Sottos, N. and White, S. (2009). Local Strain Concentrations in a Microvascular Network, *Experimental Mechanics*[Internet]. Available at: <http://dx.doi.org/10.1007/s11340-009-9299-5> (accessed January 23, 2010).
55. Lee, J.Y., Buxton, G.A. and Balazs, A.C. (2004). Using Nanoparticles to Create Self-healing Composites, *Journal of Chemical Physics*, **121**(11): 5531–5540.
56. Gupta, S., Zhang, Q., Emrick, T., Balazs, A. and Russell, T. (2006). Entropy-Driven Segregation of Nanoparticles to Cracks in Multilayered Composite Polymer Structures, *Nature Materials*, **5**(3): 229–233.
57. Verberg, R., Dale, A.T., Kumar, P., Alexeev, A. and Balazs, A.C. (2007). Healing Substrates with Mobile, Particle-filled Microcapsules: Designing a ‘Repair and Go’ System, *Journal of the Royal Society Interface*, **4**(13): 349–357.